Proceedings of the 2023 International Conference on Machine Learning and Automation
DOI: 10.54254/2755-2721/33/20230248

Bio-inspired soft robot with varied localized stiffness

Shikai Ou

College of Engineer, South China Agricultural University, Guangzhou, Guangdong, China, 510642

a13631433166@163.com

Abstract. Soft robots are a type of intelligent robot with high adaptability, and the majority of them are made from soft materials, so they are flexible and adaptable. The variable stiffness function of soft robots is crucial, as it can enhance the robot's adaptability, safety, and dependability. By adjusting the stiffness, the soft robot is able to maintain a stable motion state in a complex environment, reduce environmental interference, and perform human-like actions with improved target control. The elephant trunk served as inspiration for the way proposed in this study for modifying the soft robot's arm's stiffness. By changing the insertion scheme of the interference plate in a flexible manner, the robot arm can have variable bending capability, allowing it to complete a variety of work instructions given by humans and to satisfy a variety of work requirements.

Keywords: soft robotic arm, elephant trunk, variable stiffness, stiffness adjustment strategy.

1. Introduction

The soft robot arm is a high-degree-of-freedom robotic arm device that achieves very flexible movement and control via the deformation and control technologies of soft materials. Each particle or segment of the soft robot arm is often built of either flexible materials, rigid materials, or a combination of both, and is joined to the subsequent segment through a flexible hinge to form an open-loop moving chain. The soft robotic arm has a number of electric and pneumatic actuators that utilize cutting-edge artificial intelligence (AI) and machine learning (ML) techniques for pinpoint control of its movements. The soft robot arm offers greater benefits in deformation and motion control, and it can adjust to a wider range of item shapes and more complicated environments than its stiff counterpart. This has led to the soft robotic arm's widespread implementation in theoretical settings, in micro sectors like clamping, and in macro fields like deep-sea operations and medical care.

In the paragraphs to follow, an innovative method to tuning the soft manipulator arm's stiffness will be shown, one that is related to but distinct from the currently-used tuning techniques, thereby giving future researchers greater flexibility.

2. Literature review

Theory serves as the guide for practice, while practice is guided by theory [1]. In their 2020 paper, Gina Olson et al. proposed a quasi-static model based on Euler-Bernoulli beam theory, and verified the practical application of this model under two conditions of self-stress and external load bending [2-3]. They demonstrated that physical models are not necessary for the design and verification process of soft

© 2023 The Authors. This is an open access article distributed under the terms of the Creative Commons Attribution License 4.0 (https://creativecommons.org/licenses/by/4.0/).

DOI: 10.54254/2755-2721/33/20230248

robots when carried out by computer programs. For future research based on induction and refinement, this paper gives higher-level and more practical theoretical direction that may be applied to a wide range of related designs. Prior to this, researchers had been trying to finish the design of soft robotic arms by drawing inspiration from the movement principle of animals or specific organs within organisms. Soft arms and suction cups, for instance, have similar shapes because they were inspired by the design and muscle structure of octopus claws by Barbara Mazzolai et al. [4]. Using specialized wire laying, they created a "octopus whisker-shaped" soft framework with segments of varying stiffness from base to tip. The macroscopic phenomena is that the tentacles bend to varying degrees under the same electric drive, allowing for a tighter wrap around the target. This is the success of the soft robotic arm during close-range maneuvers.

To give them some of the desirable properties of biological organisms like adaptability, stability, versatility, and agility [5], the designers of such biologically inspired soft robotic arms often have to think completely differently about new strategies, new modes of motion, and new ways of sensing or driving. Researchers have been working tirelessly to overcome the obstacles that prevent robots with soft robot arms from functioning in harsh conditions and complex terrain [6-7]. Soft robotic arms have been used in deep-sea oil collection operations, for instance, by Kevin C. Galloway et al. to clear the seafloor of organisms before constructing oil recovery infrastructure [8]. A gentle mechanical claw has been devised to snag aquatic foes. It looks like a regular toilet brush because the front of the "claw" is made out of a sponge-like material while the back is made out of a brush-like structure. However, working on the seafloor with such a grounded design is helpful for marine life conservation since the soft claw does not kill creatures when it is picked up and transferred because the rigidity of the claw is not continuous from the root to the tip. But as medicine has advanced, minimally invasive surgery has emerged as a preferred method, meaning patients may no longer need to be disemboweled to have surgery. This is excellent news for patients, since it increases the likelihood of a successful outcome. With the advent of this new era of theory, the soft robotic arm also made its way into the operating room. When a hose is inserted into the heart from the outside of the human body, it must have varying degrees of stiffness in different sections to avoid organ obstruction and successfully reach the target surgical site in the heart. This is why the soft robotic arm developed by Yin Zhang et al. is expected to be able to handle minimally invasive cardiac surgery in the future [9]. The hook-back effect requires a small radius of curvature at the tip, while a larger radius at the root is necessary for unobstructed passage into and out of the hose.

The above demonstrates the benefits of the soft robotic arm and its increasing popularity in a number of applications. Despite the soft robotic arm's adaptability in terms of both form and function, "variable stiffness" remains a ubiquitous and crucial component of many designs. Octopus tentacles and elephant trunks, for example, have long been ideal bionic objects for the construction of soft robotic arms because of their exceptional performance of changeable stiffness. The trunk is the elephant's most sensitive organ, and it's used for a wide variety of tasks throughout the day. It can be curled inward to wrap around and grip heavy objects, or it can be bent so that the tip of the nose reaches higher than the head by first convex and then concave. The trunk's overall rigidity changes as we move; its various segments have varying curvature radii; and the trunk's robust musculature allows for gradual changes in rigidity.

3. Materials and methods

3.1. Trunk observation

The design of a bionic soft robot arm starts with observing the object to be modeled. The trunk has a flexible, variable stiffness. We used the camera to capture the left view of an elephant's trunk when it is bent upward, as shown in Figure 1(A). The feature is that there is a critical point near the tip of the trunk where the bending direction changes and the radius of curvature is theoretically infinite. When shooting, the direction of the camera should be as perpendicular as possible to the plane where the center line of the elephant trunk is located, so as to facilitate the next step of describing the curve track of the object's nose. In order to visually describe the changes of curvature in different parts of the trunk, a one-

DOI: 10.54254/2755-2721/33/20230248

dimensional coordinate system O-l was established with the root of the trunk as the origin and the direction of the trunk after it was fully expanded into a straight line as the l-axis, as shown in Figure 1(B). Set the curvature radius ρ as the longitudinal coordinate and combine with the l-axis to form the lOρ-drawing plane, forming the $\rho - l$ diagram of the trunk curvature with respect to the length from the origin. After sampling the trunk, the radius of curvature of each sampling point is calculated and marked on the $\rho - l$ diagram, and finally connected with a smooth curve. The sampling and mapping results will be shown in "3.1 Trunk behavior".

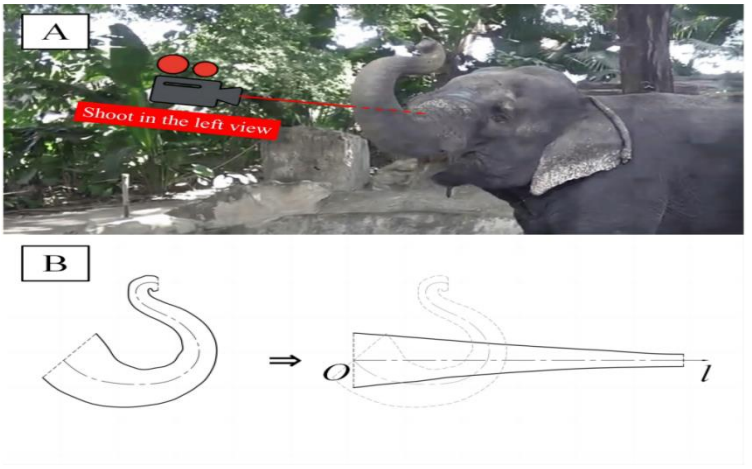

Figure 1. The upcurved curvature of the trunk (original). (A) Shoot with the camera on the left side of the elephant. (B) Trace points and draw the plot, expand the center line into a straight line, and establish a one-dimensional linear coordinate system.

3.2. Bio-inspired stiffness regulation method

Most significantly, this study led to the development of a soft robot arm equipped with an interference plate. Figure 2 depicts the three main parts of the system: the soft pneumatic actuator (SPA), the clip, and the interference plates. Everything is produced via 3D printing. To insert the interference plate, the SPA body is carved with numerous tiny grooves, but these grooves also serve another purpose: they provide a stable structural foundation for the soft robot arm's deformation by concentrating the internal stress caused by the arm's deformation. The clip is immobile throughout robot arm motion because it is permanently fastened to the gas driving force source and is a stable object in terms of the global coordinate system. The whole robotic arm is similar to the cantilever beam in the Mechanics of Materials, with a similar way of fixing the boundary.

DOI: 10.54254/2755-2721/33/20230248

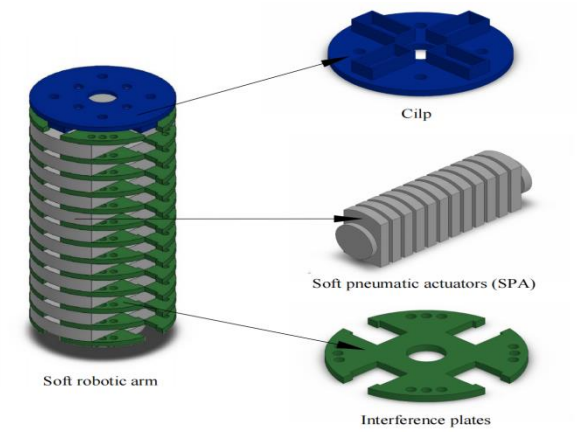

Figure 2. Structure of flexible manipulator arm with adjustable stiffness (original). (The soft manipulator is assembled by a soft pneumatic actuator (SPA), interference plates and a clip.)

The soft manipulator's stiffness adjustment approach relies on the insertion number and position arrangement of interference plates. In Figure 3, we can see that the very top of the entire robot arm is a fixed clip, so we've decided to divide this section of the device and call it the base. Starting at the bottom, every set of three interference plates constitutes a deformation zone, making a total of four zones throughout the robot arm. We conduct experimental tests on four distinct methods for installing interference panels. Strategy 1 involves inserting interference plates into each of three slots (represented by [1,1,1]); Strategy 2 involves inserting no interference plates into the center slot (represented by [1,0,1]), with both strategies focusing on the deformation area nearest the base. For example, [0,1,1] indicates that no interference board is inserted into the slot closest to the base, while [0,0,1] indicates that only the slot farthest away from the base contains interference board. Given that the first deformation zone serves as a template for the subsequent three deformation zones, we know exactly how the interference plates will be distributed among the four insertion strategies. The number of interference plates in strategy 1 is the highest, while the number of interference plates in strategy 4 is the lowest. Empirical speculation suggests that Strategy 1 results in the most flexible manipulator arm, whereas Strategy 4 results in the most rigid. In order to regulate the stiffness of the manipulator arm quantitatively, "3.2 Bio-inspired stiffness regulation method" will conduct tests to determine the optimal amount of interference plates to insert and how to distribute them across the arm's working range.

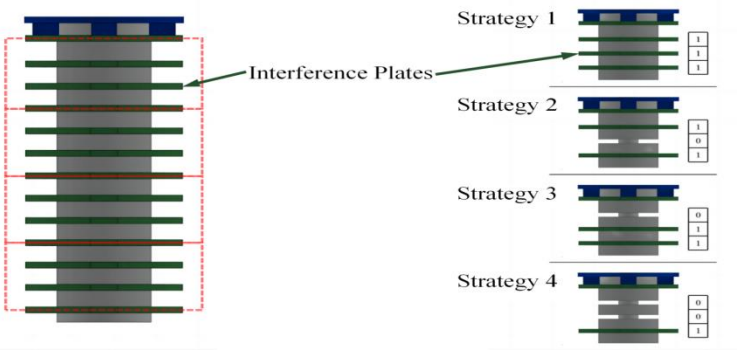

Figure 3. Area division and chip strategy (original). We divide the soft robot arms into four deformation zones. Here we propose four insertion strategies 1 to 4. The "1" in the box on the right of the figure means inserting the interference board, and "0" means not inserting the interference board.

DOI: 10.54254/2755-2721/33/20230248

3.3. Deformation behavior measurement

The stiffness of the manipulator arm, the insertion strategy of the interference plate, and the applied air pressure must be determined so that the degree of achievement of design goals and performance of the stiffness adjustment strategy of this soft manipulator arm can be evaluated. Using a computer for data recording, data processing, and drawing procedures, the research results are analyzed in terms of their design. Clarifying the methodologies used to measure the aforementioned three physical quantities—rigidity, interference plate insertion strategy, and air pressure—has become an essential and necessary step. To begin, the radius of the bend in the manipulator, denoted by, has a positive relationship with the stiffness K of the manipulator. A bigger curvature with a lower radius of curvature means less stiffness and a greater capacity for bending deformation. Therefore, the stiffness of the robotic arm may be determined by its radius of curvature; so, in the subsequent tests, the focus will be on the more easily measurable radius of curvature. There is no difficulty in measuring the applied air pressure because the value may be read directly from the pressure sensor at the power source, and a technique for inserting the interference plates has been provided in the previous section on naming conventions. There is now a realistic and scientific means of calibrating the three most important physical quantities.

4. Results and discussion

4.1. Trunk behavior

Figure 4 displays the relationship between the observed curvature radius of the elephant trunk (as detailed in "2.1 Trunk observation") and the distance between the trunk and the coordinate origin. The subsequent findings are in accord with this experimental phenomenon.

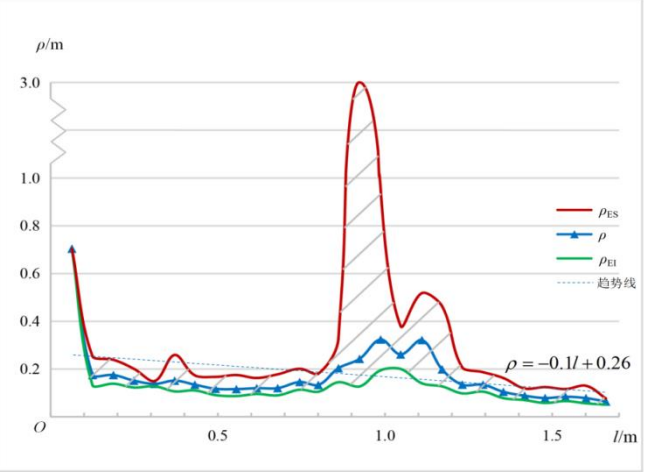

Figure 4. ρ − l diagram of the trunk (original). The experiment was repeated for many times. The blue dots and curve represented the average value of the experimental results, the blue lines represented the change trend of the average value, and the red and green curves respectively represented the upper and lower deviations of the experimental results.

First, from the trend of the trend line and the slope of the function, it can be seen that ρ gradually decreases on the whole with the increase of l (except at the turning point near $l = 0.9$ m). The curvature radius of the trunk root is larger, and the stiffness is larger. The closer to the tip of the nose, the more curved it is, and we found that the closer to the external object to be touched, the more flexible the position of the elephant's nose. This is a common phenomenon in the evolution of organisms, such as the toes of many mammals and the legs of many insects. The human hand is the most commonly used organ for grasping objects, so it has more freedom than the arm. The feet need to be in constant contact with the ground and adapt to different terrain, so they are more flexible than the thighs, which are closer to the human core. This law suggests that when we need to use a soft robot arm to adjust the stiffness

DOI: 10.54254/2755-2721/33/20230248

strategy in the future, we should first consider the scheme of decreasing stiffness from the root to the tip, which can increase the success rate of the design.

Second, when $l = 0.9$ m, the radius of curvature suddenly rises to the highest point, then drops rapidly after a short period of fluctuation, and then recovers to a low level after a period of time and continues to the tip of the nose, especially the speed of the rise and fall of the upper deviation line is extremely fast, and the rise and fall of the mean line is not as steep as that of the upper deviation line, but an obvious trend can be seen. This is because the bend of the trunk changes, and the critical point regularly appears near the tip of the nose. In theory, when the concave curve is transiting to the convex curve, there will inevitably be a point with an infinite radius of curvature, and the blue curve should pass through the zero point, but in practice, when the elephant lifts its trunk to the same height, it will fine-tune the stiffness of the local muscles of the nose, so the actual curve does not pass the l axis and there is a certain positive error. The tolerance range has been represented in Figure 4 by a shaded line, that is, the part between the red curve and the green curve.

4.2. Bio-inspired stiffness regulation method

As described in "2.3 Deformation behavior measurement", exploring the method of bionic stiffness adjustment requires the determination of the quantitative relationship between the stiffness (measured by the radius of curvature) and the interference plate insertion strategy. We made the computer designed model into a real object, as shown in Figure 5. Four groups of soft robot arms were set up in the experiment by applying four interference plate insertion strategies, respectively. The curvature radius of the robot arm under each deformation condition was measured under the same pressure of pneumatic force, and the measured experimental results were plotted on the $\rho - AS$ diagram (AS represents the assembly strategy). The results are shown in Figure 6. The following results can be obtained from the figure.

Figure 5. A physical model of a flexible manipulator with adjustable stiffness (original).

DOI: 10.54254/2755-2721/33/20230248

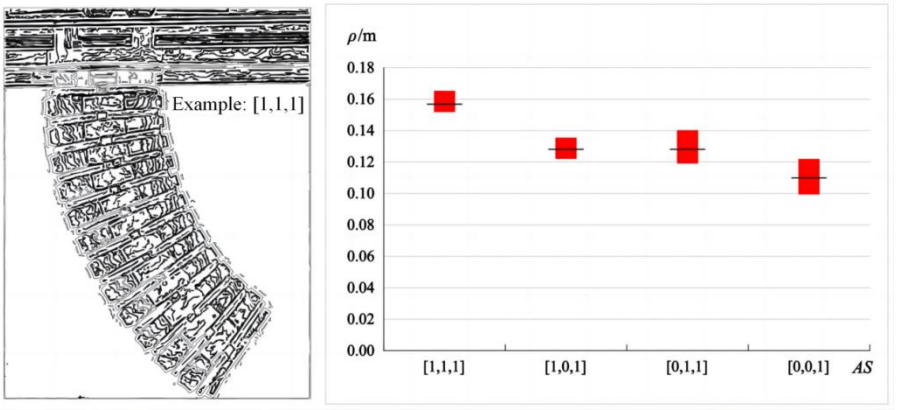

Figure 6. Experimental verification of bionic stiffness adjustment method (original). The curvature radius of the soft manipulator arm under four insertion strategies ([1,1,1], [1,0,1], [0,1,1] and [0,0,1]) at constant pressure $P = 100\,kPa$. The experiment was repeated for many times. The range of the distribution of the experimental results was represented by a red rectangle block, and the black straight line through the rectangle block represented the average value of the data.

First, by tracking the rise and fall of the black line, we may deduce that the bending degree of the mechanical arm increases as the number of interference plates introduced into a deformation zone reduces. Each SPA groove is analogous to a human arm joint; inserting an interference plate into a groove limits the robot arm's rotational range at that groove, much like injecting a medication into a human arm joint limits its range of motion. The stiffness of the arm as a whole will increase if all its "joints" are constrained, and vice versa if the number of constrained grooves is decreased. Therefore, the experimental results are genuine, valid, and reliable, as they correspond to the experimental hypotheses.

Second, the experimental results' tolerance grows as one reads along the AS coordinates from left to right. The reason for this phenomenon seems to be caused by the reduction in the number of interference plates inserted, but compared with the two groups of mechanical arms with the same number of interference plates inserted [1,0,1], the tolerance of the latter is larger, so the size of the experimental error is more likely to depend on the density of the number of interference plates near the root, which is reflected in Figure 6 that "1" appears earlier. The tolerance will be smaller. The logic behind this is that the slot's motion state is relatively stable and controllable when the interference plates are attached, but more free when they are removed. Since reducing the amount of interference plates installed can improve the robot arm's bending capacity but also makes the structure more vulnerable to interference from the outside environment, the two exhibit a contradictory relationship. Therefore, when building a flexible robot arm with tunable stiffness, it is important to accurately assess the potential benefits and drawbacks, and choose an acceptable insertion approach in light of the robot arm's real flexibility needs.

5. Conclusion

Adjusting the rigidity of a soft manipulator arm is discussed in this study. This paper begins by explaining why it's so crucial for soft robotic arms to have adjustable stiffness. It then uses observations of elephant trunks to learn more about the characteristics of stiffness change, which in turn inspired the development of a new technique for adjusting the bending degree and bending ability of mechanical arms by switching the insertion mode of an interference plate. The experimental results reveal that the stiffness of the soft robot arm decreases with the number of added interference plates, but the control complexity also rises. Different segments of the same arm can have varying stiffness due to the placement and combination of various insertion modes. Future studies will have the opportunity to carefully weigh and compare this stiffness adjustment technique with others, such as those that involve altering the wire layout, the air pressure, the material qualities, etc. The focus of future research will

DOI: 10.54254/2755-2721/33/20230248

shift toward practical applications, with the goal of employing it in a number of various contexts at work, refining it in the context of those contexts, and carrying out targeted design to satisfy the larger application needs.

References

[1] Taofen Z. On Practice[M]. Beijing, China: People's Publishing House, 1940: 300.
[2] Olson G, Hatton R L, Adams J A, et al. An Euler–Bernoulli beam model for soft robot arms bent through self-stress and external loads[J]. International Journal of Solids and Structures. 2020, 207: 113-131.
[3] Zhang X, Thompson D, Sheng X. Differences between Euler-Bernoulli and Timoshenko beam formulations for calculating the effects of moving loads on a periodically supported beam[J]. Journal of sound and vibration. 2020, 481: 115432.
[4] Mazzolai B, Mondini A, Tramacere F, et al. Octopus-Inspired Soft Arm with Suction Cups for Enhanced Grasping Tasks in Confined Environments[J]. Advanced Intelligent Systems. 2019, 1(6): 1900041.
[5] Rolf Pfeifer M L F. Self-Organization, Embodiment, and Biologically Inspired Robotics[J]. Science. 2007.
[6] Murphy R R. Disaster Robotics[M]. The MIT Press, 2014.
[7] Bogue R. Disaster relief, and search and rescue robots: the way forward[J]. Industrial Robot: the international journal of robotics research and application. 2019, 46(2): 181-187.
[8] Galloway K C, Becker K P, Phillips B, et al. Soft Robotic Grippers for Biological Sampling on Deep Reefs[J]. Soft Robotics. 2016, 3(1): 23-33.
[9] Zhang Y, Liao J, Chen M, et al. A multi-module soft robotic arm with soft actuator for minimally invasive surgery[J]. The International Journal of Medical Robotics and Computer Assisted Surgery. 2023, 19(1).